Molecular Diversity (2022) 26:1995–2009
https://doi.org/10.1007/s11030-021-10310-7

ORIGINAL ARTICLE

Design and synthesis of phenoxymethybenzoimidazole incorporating different aryl thiazole-triazole acetamide derivatives as α-glycosidase inhibitors

Anita Nasli Esfahani[1] · Aida Iraji[2,3] · Amir Alamir[1] · Shahram Moradi[1] · Mohammad Sadegh Asgari[4] · Samanesadat Hosseini[5] · Somayeh Mojtabavi[6] · Ensieh Nasli-Esfahani[7] · Mohammad Ali Faramarzi[6] · Fatemeh Bandarian[7] · Bagher Larijani[8] · Haleh Hamedifar[9] · Mir Hamed Hajimiri[10] · Mohammad Mahdavi[8]

Received: 12 July 2021 / Accepted: 1 September 2021 / Published online: 13 September 2021

Abstract

A novel series of phenoxymethybenzoimidazole derivatives (**9a-n**) were rationally designed, synthesized, and evaluated for their α-glycosidase inhibitory activity. All tested compounds displayed promising α-glycosidase inhibitory potential with IC_{50} values in the range of 6.31 to 49.89 μM compared to standard drug acarbose ($IC_{50} = 750.0 \pm 10.0$ μM). Enzyme kinetic studies on **9c**, **9g,** and **9m** as the most potent compounds revealed that these compounds were uncompetitive inhibitors into α-glycosidase. Docking studies confirmed the important role of benzoimidazole and triazole rings of the synthesized compounds to fit properly into the α-glycosidase active site. This study showed that this scaffold can be considered as a highly potent α-glycosidase inhibitor.

Keywords α-Glycosidase · Synthesis · Benzimidazole · Triazole-acetamide · Enzyme inhibition

Introduction

Diabetes mellitus (DM) recognizes as one of the most extensive global health emergencies in the twenty-first century affecting more than 400 million people worldwide, and it is estimated that the number will reach around 600 million by 2035 [1].

DM is a chronic metabolic disorder leading to hyperglycemia with the problem in the metabolism of carbohydrates, lipids, and proteins [2]. DM is categorized into two major sub-types type 1 DM and type 2 DM. Type 1 DM is an autoimmune disorder that the immune system mistakenly attacks the β cells of the pancreas which reduces or impairs the production of insulin [3]. Type 2 DM, with more than

✉ Mir Hamed Hajimiri
h.hajimiri@nanoalvand.com

✉ Mohammad Mahdavi
mahdavi.chem@gmail.com

1 Department of Chemistry Tehran North Branch, Islamic Azad University, Tehran, Iran

2 Stem Cells Technology Research Center, Shiraz University of Medical Sciences, Shiraz, Iran

3 Central Research Laboratory, Shiraz University of Medical Sciences, Shiraz, Iran

4 Department of Chemistry, Iran University of Science and Technology, Tehran, Iran

5 Department of Pharmaceutical Chemistry, School of Pharmacy, Shahid Beheshti University of Medical Sciences, Tehran, Iran

6 Department of Pharmaceutical Biotechnology, Faculty of Pharmacy and Biotechnology Research Center, Tehran University of Medical Sciences, Tehran, Iran

7 Diabetes Research Center, Endocrinology and Metabolism Clinical Sciences Institute, Tehran University of Medical Sciences, Tehran, Iran

8 Endocrinology and Metabolism Research Center, Endocrinology and Metabolism Clinical Sciences Institute, Tehran University of Medical Sciences, Tehran, Iran

9 CinnaGen Medical Biotechnology Research Center, Alborz University of Medical Sciences, Karaj, Iran

10 Nano Alvand Company, Tehran University of Medical Sciences, Avicenna Tech Park, 1439955991 Tehran, Iran

90–95% of the cases, characterized by insulin resistance in target tissues, mainly skeletal muscle, adipose tissue, and liver. To fight back against insulin resistance, β-cells overwork to produce more insulin, and gradually the β-cells of the pancreas are destroyed, and insulin secretion is reduced and diminished [4]. DM is associated with a lot of complications including heart disease, stroke, blindness, renal failure, foot amputation, and even death [5]. The main medical approach to control the progress of DM and its complications focuses on the reduction of the postprandial glucose level in blood via regulating and/or inhibiting carbohydrate hydrolytic enzymes [6, 7].

α-Glycosidase (EC.3.2.1.20) is an important membrane-bound intestinal hydrolytic enzyme playing a vital role in the digestion of carbohydrates [8–10]. It hydrolyzes oligosaccharides, trisaccharides, and disaccharides to glucose and other monosaccharides at their non-reducing ends (α-glycosidic bonds) after hydrolysis of polysaccharides to oligosaccharides by α-amylase. As a result, α-glycosidase inhibitors transfer the undigested carbohydrate into the distal part of the small intestine and colon, delay the process of carbohydrate absorption in the gastrointestinal tract, and reduce postprandial hyperglycemia [4, 11, 12].

Acarbose, miglitol, and voglibose used as α-glycosidase inhibitors, mostly obtained from natural sources due to multiple complicated syntheses steps [13]. Also, administration of these inhibitors can bring undesirable side effects including serious gastrointestinal disorders such as diarrhea and flatulence. For this reason, several research groups have investigated the efficiency of small molecules possessing potent α-glycosidase inhibitory potential including imidazole [14], pyrazoles [15], quinazolinone [16], isatin[17], pyrimidine[18], xanthone [19], azole [20], and macrocyclic compounds [21, 22].

Considering the important properties of triazoles such as easy synthetic protocol and promising anti-diabetic properties [23] as well as imidazole and its derivatives as one of the most important nitrogen-containing heterocyclic scaffolds in medicinal chemistry [24, 25], the current study is conducted to evaluate anti-α-glycosidase properties of newly designed phenoxymethybenzoimidazole coupled different thiazole-triazole acetamide (**9a-n**) derivatives. Kinetic studies of the most potent compounds were also performed to evaluate their inhibition pattern against α-glycosidase.

Results and discussion

Rational study of the present work

Benzimidazole-based compounds possess a wide range of pharmaceutical and biological activities, especially α-glycosidase inhibition [26]. Zawawi et al. screened a novel series of thiourea derivatives bearing benzimidazole with IC_{50} values between 35.83 and 297.99 μM which was better than the standard drug acarbose with $IC_{50} = 774.5$ μM. According to molecular docking study of the most potent compound (**A,** Fig. 1), imidazole moiety formed hydrogen bond with Glu 276, and phenyl rings showed arene–arene interaction with residue Phe 157 of the α-glycosidase active site [27]. In 2019, Taha et al. evaluated novel benzimidazole-based oxadiazole derivatives for their in vitro anti-α-glycosidase activity. Among the screened analogs, compound **B** showed excellent inhibitory potential with an IC_{50} value of 2.6 ± 0.1 μM compared with acarbose ($IC_{50} = 38.45 \pm 0.80$ μM). According to the structure–activity relationship (SAR), the substitution of methyl and methoxy moiety on phenyl ring recorded hydrophobic interaction and decreased inhibitory potential significantly [28]. In another study, Rahim et al. introduced benzimidazole bearing bis-Schiff bases as α-glycosidase inhibitors. All derivatives displayed moderate to good inhibitory potential with an IC_{50} ranging from 2.20 to 88.60 μM compared with standard drug acarbose ($IC_{50} = 38.45$ μM). The great potential of analog **C** ($IC_{50} = 2.20 \pm 0.1$ μM) mainly seems to be due to methoxy and hydroxyl groups presented on two phenyl rings which might be involved in hydrogen bonding with the active site (Fig. 3)[29].

It was found that the benzimidazole ring as the basic skeleton of compounds was responsible for this promising α-glycosidase inhibition.

Triazole acetamide moiety has been already identified with α-glycosidase inhibitory potential. In this context, Wang et al. reported xanthone-triazole acetamide hybrids **D** with significant anti-α-glycosidase activities. Analog **D** showed high activities in promoting glucose uptake and low toxicity to the human normal hepatocyte cell line (Fig. 1) [30]. Another set of benzimidazole-1,2,3-triazole hybrids were screened as α-glycosidase inhibitors. In this respect, compound **E** depicted an IC_{50} value of 25.2 ± 0.9 μM in comparison with standard drug acarbose ($IC_{50} = 750.0 \pm 12.5$ μM) [31]. In 2021, another set of indolinone-substituted phenoxy methyltriazole was synthesized and the most potent derivative in this set (Compound **F**) showed around a 46-fold improvement in the inhibitory activity against α-glycosidase, compared with acarbose [17].

Another interesting pharmacophore to design potent α-glycosidase inhibitors is aryl thiazole substituent. Compound **G** ($IC_{50} = 2.2$ μM) with *p*-methoxy pendant displayed strong α-glycosidase inhibitory activity that fulfilled the conformational requirement to fit well in the active site of the enzyme [32]. A set of arylthiazole-pyridine derivatives were also screened as possible α-glycosidase inhibitors (Compound **H**). All analogs exhibited potent inhibition in the range of 1.40 to 236.10 μM compared to the standard

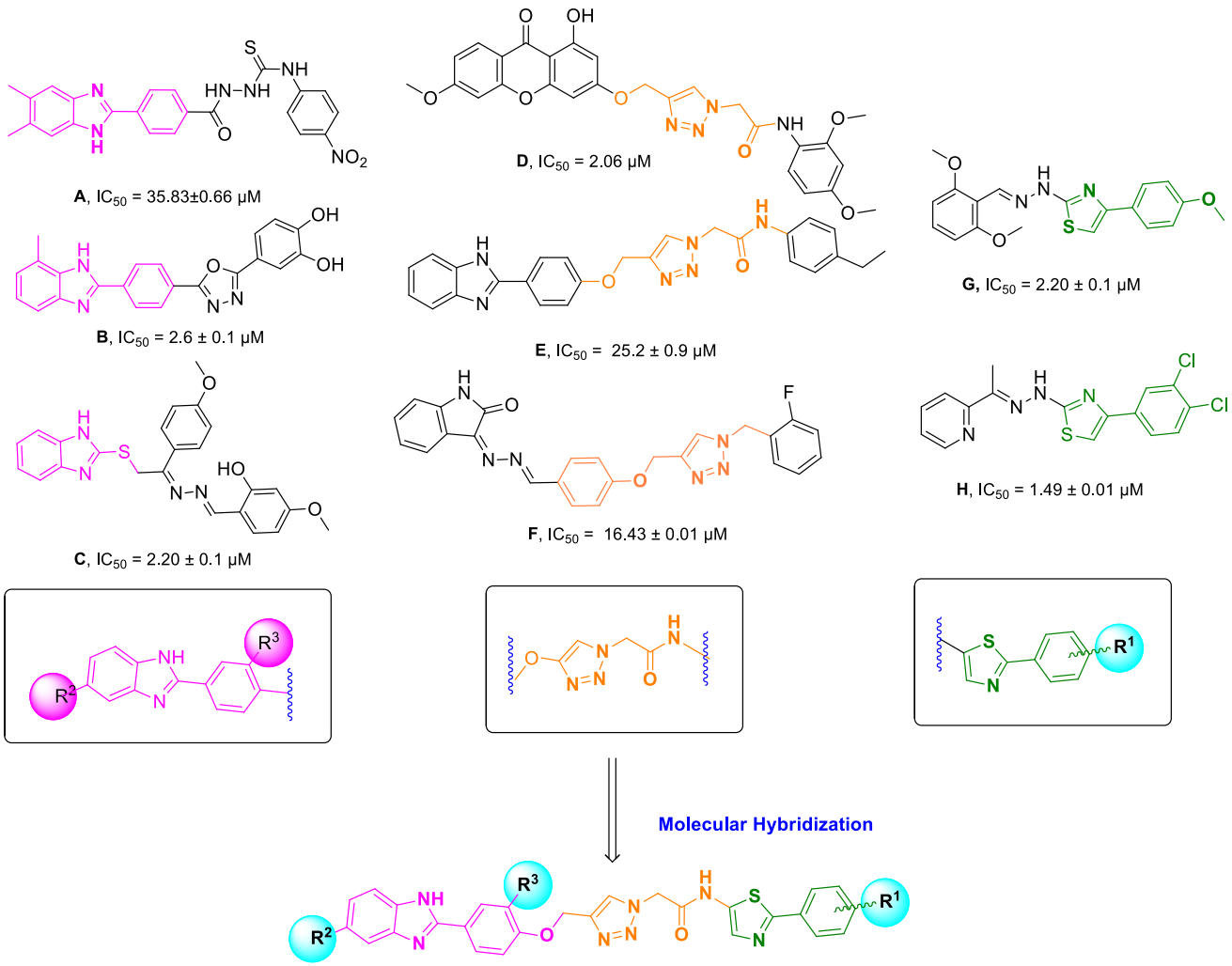

Fig. 1 Rational design of phenoxymethybenzoimidazole coupled different aryl thiazole-triazole acetamide

acarbose ($IC_{50} = 856.45 \pm 5.60$ µM) owing to interactions with Pro309, Phe157, and Asn347 residues [33].

Keeping the above-mentioned importance of benzimidazole, triazole, and aryl thiazole moieties in the design of new α-glycosidase inhibitors, herein, the hybridization strategy of these pharmacophores was applied to deign novel phenoxymethybenzoimidazole bearing different aryl thiazole-triazole acetamide derivatives. Various substituents were performed on benzimidazole, triazole, and aryl thiazole moieties to define beneficial SARs as α-glycosidase inhibitors.

Chemistry

The synthesis of compounds **9a-n** is schematically presented in scheme 1. The methyl group of commercially available acetophenone derivatives (**1**) was reacted with n-bromosuccinimide in the presence of *p*-toluenesulfonic acid to give α-bromoacetophenone derivatives (**2**). Then compound **2** reacted with thiourea in ethanol to give 4-arylthiazol-2-amines (**3**). The reaction of intermediate **3** with 2-chloroacetyl chloride gave compound **4**. On the other hand, different phenylenediamines **6** reacted with 4-(prop-2-ynyloxy)benzaldehyde derivatives **7** in the presence of $Na_2S_2O_5$ in DMF at 100 °C to give the corresponding compound **8**. The target compounds **9a-n** were synthesized via click reaction of compound **5** and freshly prepared azide derivatives in the presence of the catalytic amount of triethylamine (Et_3N) in H_2O and t-BuOH (1:1) at RT [34–36].

In vitro α-glycosidase enzymatic assay

The fourteen derivatives prepared herein (**9a-n**) were subjected to in vitro α-glycosidase inhibition. According to the results reported in Table 1, all compounds showed exceptionally high potency against α-glycosidase with an IC_{50} value ranging from 6.31 to 49.89 µM which is significantly lower than that of acarbose as the positive control ($IC_{50} = 750.0 \pm 10.0$ µM). Compound **9g** ($IC_{50} = 6.31$ µM;

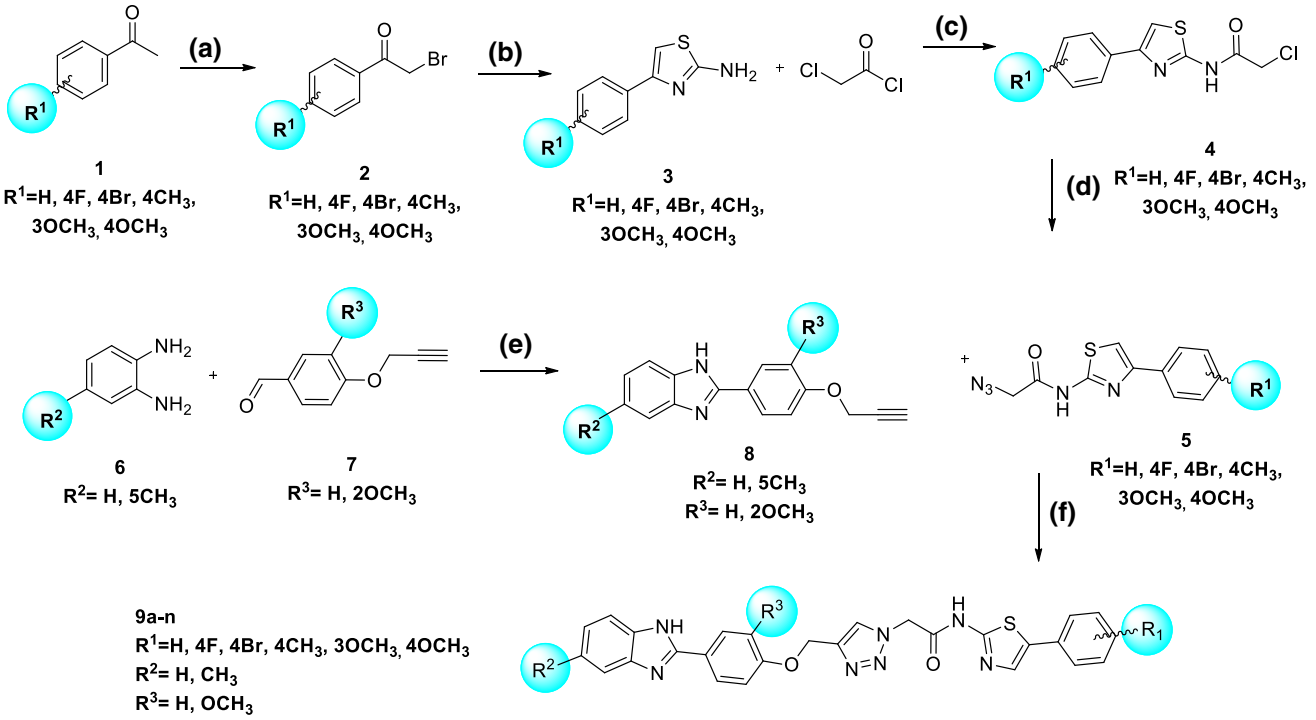

Scheme 1. Reagents and conditions for the synthesis of **9a-n**: **a** *p*-$MeC_6H_4SO_3H$, NBS, CH_3CN, reflux, 2 h; **b** thiourea, EtOH, reflux; **c** Et_3N, CH_2Cl_2, room temperature, 24 h; **d** NaN_3, Et_3N, H_2O/t-BuOH, RT, 1 h; **e** DMF, $Na_2S_2O_5$, 100 °C, 2 h; **f** $CuSO_4.5H_2O$, sodium ascorbate, RT, 24–48 h

$R^1=H$, $R^2=H$, $R^3=OCH_3$), **9m** ($IC_{50}=8.30$ μM; $R^1=4CH_3$, $R^2=CH_3$, $R^3=H$), and **9c** ($IC_{50}=8.88$ μM; $R^1=4Br$, $R^2=H$, $R^3=H$) showed the highest activity among this series of compounds. To better understand the SAR, synthetic compounds were divided into six groups.

Evaluating the effect of R^1 moiety on phenoxymethybenzoimidazole derivatives ($R^2=H$ and $R^3=H$)

According to the obtained results, it can be seen that **9a** as an unsubstituted compound ($R^1=H$, $R^2=H$, $R^3=H$) demonstrated an IC_{50} value of 19.12 μM with around 39 times improvement in potency compared to that of acarbose as a positive control. Substitution of fluorine as a small electron-withdrawing group at R^1 (**9b**) decreased the inhibitory potency compared to **9a**. However, the replacement of fluorine (**9b**) with bromine (**9c**) as more lipophile and bulkier halogen group significantly improved the α-glycosidase inhibition with around twofold increase in the inhibitory potency compared to **9a**. Considering the substitution of electron-donating moieties, it can be seen that the presence of a moderate electron-donating group at the *para* position led to the relatively strong inhibitory activity (**9d**; $R^1=4CH_3$, $R^2=H$, $R^3=H$; $IC_{50}=9.53$ μM). Replacement of the methyl group with a strong electron-donating group (MeO) on the benzoimidazole ring significantly reduced the α-glycosidase inhibition. This trend can be seen in **9e** ($R^1=4OCH_3$, $R^2=H$, $R^3=H$; $IC_{50}=35.11$ μM) and **9f** ($R^1=3OCH_3$, $R^2=H$, $R^3=H$; $IC_{50}=15.01$ μM).

Evaluating the effect of R^1 moiety on phenoxymethybenzoimidazole derivatives while $R^2=H$ and $R^3=OCH_3$

In cases of **9g-j**, it can be seen that the **9g** ($R^1=H$, $R^2=H$, $R^3=OCH_3$) recorded the best inhibitory activity among all derivatives with an IC_{50} value of 6.31 μM. As can be understood in **9h** ($R^1=4Br$, $R^2=H$ and $R^3=OCH_3$; $IC_{50}=26.97$ μM), **9i** ($R^1=4CH_3$, $R^2=H$ and $R^3=OCH_3$; $IC_{50}=49.89$ μM), and **9j** ($R^1=4OCH_3$, $R^2=H$ and $R^3=OCH_3$; $IC_{50}=11.25$ μM), any substitution in this set dramatically reduced the α-glycosidase inhibitory activity. The least potent derivatives in this set were **9i** possessing *para*-CH_3 at R^1 with IC_{50} value of 49.89 μM still demonstrating 15-fold increasing in potency comparing with acarbose.

Table 1 In vitro α-glycosidase inhibitory activity of novel phenoxymethybenzoimidazlo coupled different aryl thiazole-triazole acetamide derivatives (**9a–n**)

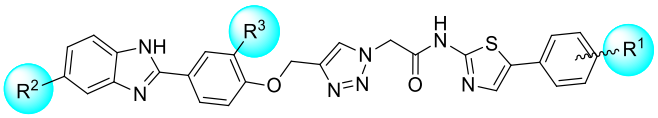

Compounds	R^1	R^2	R^3	IC_{50} (μM)[a]	Concentrations of Precipitation (μM)
Acarbose				750.0 ± 10.0	-
9a	H	H	H	19.12 ± 0.08	750, 300, 150, 100
9b	4F	H	H	31.56 ± 0.12	750, 300, 150, 100
9c	4Br	H	H	8.88 ± 0.07	750, 300, 150, 100
9d	$4CH_3$	H	H	9.53 ± 0.12	750, 300, 150, 100
9e	$4OCH_3$	H	H	35.11 ± 0.07	750, 300, 150, 100
9f	$3OCH_3$	H	H	15.01 ± 0.18	750, 300, 150, 100
9g	H	H	OCH_3	6.31 ± 0.03	750, 300, 150, 100
9h	4Br	H	OCH_3	26.97 ± 0.25	750, 300, 150, 100
9i	$4CH_3$	H	OCH_3	49.89 ± 0.09	750, 300, 150, 100
9j	$4OCH_3$	H	OCH_3	11.25 ± 0.15	750, 300, 150, 100
9k	H	CH_3	H	12.67 ± 0.05	750, 300, 150, 100
9l	4Br	CH_3	H	14.20 ± 0.21	750, 300, 150, 100
9m	$4CH_3$	CH_3	H	8.30 ± 0.16	750, 300, 150, 100
9n	$4OCH_3$	CH_3	H	24.19 ± 0.1	750, 300, 150, 100

[a] Data represented in terms of mean ± SD.

Evaluating the effect of R^1 moiety on phenoxymethybenzoimidazole derivatives while $R^2 = CH_3$ and $R^3 = H$

In this set of compounds (**9k-n**), the most active compound was **9m** ($R^1 = 4CH_3$, $R^2 = CH_3$ and $R^3 = H$) with an IC_{50} value of 8.30 μM. Disappointingly replacement of $4CH_3$ in **9m** with $4OCH_3$ (**9n**) moiety significantly lessened the inhibitory activity. Although the substitution of *para*-bromine as an electron-withdrawing group (**9l**, $IC_{50} = 14.2 \pm 0.21$ μM) led to around twofold improvement of α-glycosidase inhibitory activity compared with **9n**, the inhibitory potency did not improve compared with $4CH_3$ (**9m**) counterpart.

Evaluating the inhibitory effect on phenoxymethybenzoimidazole while $R^1 = 4CH_3$ moiety.

On the other hand, the potency of **9d**, **9i**, **9m** bearing methyl group at R^1 indicated the following order of potency so that **9m** ($IC_{50} = 8.30$ μM, $R^1 = 4CH_3$, $R^2 = CH_3$, $R^3 = H$) > **9d** ($IC_{50} = 9.53$ μM, $R^1 = 4CH_3$, $R^2 = H$, $R^3 = H$) > > **9i** ($IC_{50} = 49.89 \pm 0.09$ μM, $R^1 = 4CH_3$, $R^2 = H$, $R^3 = 2OCH_3$). It seems that substitution of OCH_3 at R^3 position in compounds bearing $4CH_3$ at R^1 deteriorated the inhibitory potency.

Evaluating the inhibitory effect on phenoxymethybenzoimidazole while $R^1 = 4Br$ moiety

Comparison of the bromine derivatives at R^1 (**9c**, **9h**, **9l**) highlighted this trend that the presence of OCH_3 pendant with strick hindrance at R^3 had a negative effect on α-glycosidase inhibition compared to the unsubstituted one.

Furthermore, the power and the position of substitution significantly affect the potency. This pattern can be seen in compounds **9c** (IC_{50} = 8.88 µM; R^1 = 4Br, R^2 = H, R^3 = H) > **9l** (IC_{50} = 14.20 µM, R^1 = 4Br, R^2 = CH_3, R^3 = H) > **9h** (IC_{50} = 26.97 µM; R^1 = 4Br, R^2 = H, R^3 = OCH_3).

Evaluating the inhibitory effect on phenoxymethybenzoimidazole while R^1 = methoxy moiety

From the screening data of **9e**, **9f**, **9j**, and **9n**, it was revealed that **9j** having $4OCH_3$ moiety at R^1 (IC_{50} = 11.25 µM; R^1 = $4OCH_3$, R^2 = H, R^3 = OCH_3) had superior inhibitory activity toward α-glycosidase in this analog followed by **9f** (IC_{50} = 15.01 µM; R^1 = $3OCH_3$, R^2 = H, R^3 = H), **9n** (IC_{50} = 24.19 µM; R^1 = $4OCH_3$, R^2 = CH_3, R^3 = H), **9e** (IC_{50} = 35.11 µM; R^1 = $4OCH_3$, R^2 = H, R^3 = H). It seems that the presence of MeO as strong and bulk electron-donating group at R^1 and R^3 in this set can improve anti-α-glycosidase activity.

Overall, it can be understood that phenoxymethybenzoimidazole bearing thiazole-triazole acetamide as the basic skeleton was responsible for this outstanding α-glycosidase inhibition.

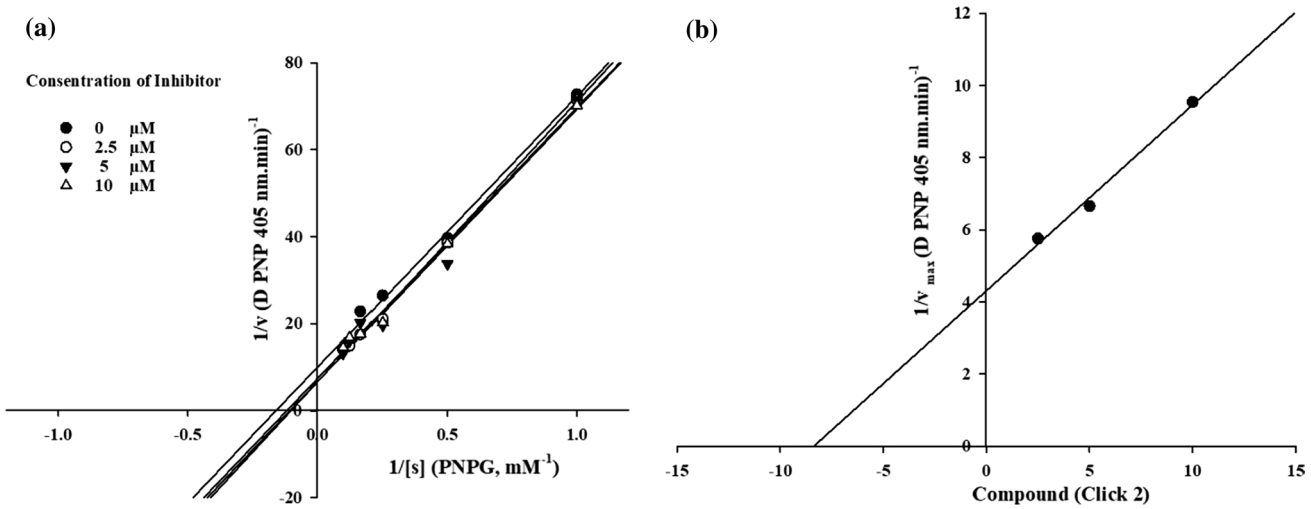

Fig. 2 Kinetics of α-glycosidase inhibition by **9c**. **a** The Lineweaver– Burk plot in the absence and presence of different concentrations of **9c**; **b** the secondary plot between $1/V'_{max}$ and various concentrations of **9c**

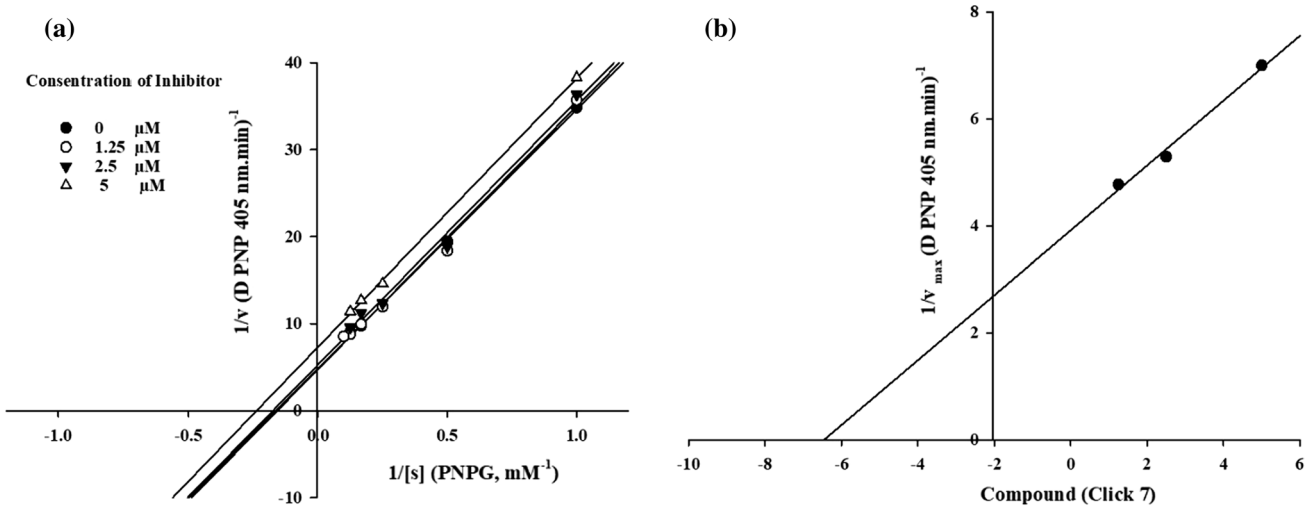

Fig. 3 Kinetics of α-glycosidase inhibition by **9g**. **a** The Lineweaver– Burk plot in the absence and presence of different concentrations of **9g**; **b** the secondary plot between $1/V'_{max}$ and various concentrations of **9g**

Enzyme kinetic studies

According to Figs. 2, 3, and S1, the Lineweaver–Burk plot showed that the K_m gradually increased and V_{max} remained unchanged with increasing inhibitor concentration indicating an uncompetitive inhibition. The results showed **9c**, **9 g**, and **9 m** bind to ES and had no binding with the free active site. Furthermore, the plots of the $1/V'_{max}$ versus different concentrations of **9c**, **9g**, and **9m** gave an estimate of the inhibition constant, K_i of 8.5, 6.3, and 8.3 µM, respectively (Figs. 2b, 3b, and Fig. S1b).

Docking analyses

Docking studies were carried out to understand the interaction modes of the most potent derivatives (**9c**, **9g,** and **9m**) in the α-glycosidase active site. First, the validation process was performed and resulted in an RMSD value of 3.41 Å. The top-scoring pose of acarbose as a crystallographic ligand (PDB ID: 5NN8) is shown in Fig. 4. Acarbose demonstrated seven H-bound interactions with Asp282, Arg600, Asp616, and His674, two Van der Waals with Trp376 and Asp404 plus one pi-alkyl interaction with Trp376.

The gold score value of **9c, 9g, 9m** plus their interactions with amino acid residues in the α-glycosidase active site is shown in Table 2. As can be seen, the order of in vitro inhibitory potency recorded well correlation with gold score values. This trend can easily be seen in **9g** as the most potent compound with an IC_{50} value of 6.31 µM, generated the highest gold score value (70.16).

3D interaction patterns of compounds **9c**, **9g**, **9m** as the best α-glycosidase inhibitors are shown in Figs. 5, 6, 7.

Overall it can be seen that benzimidazole and triazole rings can be considered as critical moieties to develop anti-α-glycosidase agents. Meanwhile, phenoxymethyl and thiazoleacetamide linkers can provide optimum length and bulkiness to properly occupy the α-glycosidase active site.

To get better inside into the conformation and orientation of each derivative into the active site compared with acarbose, the superimposed structures of all compounds are shown in Fig. 8. Assessment on superimposed structures exhibited that phenoxymethybenzoimidazole moiety of **9c** and **9g** had similar orientation in the active site and the difference in their pose came back to the substituted group at R^1. However, **9m** showed different conformation in the active site compared to **9c** and **9g** which may be due to the presence of the *para*-methyl group as well as methyl at R^1 and R^2, respectively.

Interestingly, amino-4-(hydroxymethyl)cyclohexene-triol group of acarbose was well aligned on the benzimidazole moiety of **9c** and **9g**, while methylphenyl group (R^1) of **9m** was aligned on glucopyranose of acarbose. According to docking studies, it was clear that substituted moiety at R^1 and R^2 effectively determined the conformation and pose of each ligand in the binding site as well as provided additional interactions with the active site. Although these compounds were unable to exhibit the same binding pose, they were properly fitted into the binding site and demonstrated interactions with the critical resides of the α-glycosidase active site.

Conclusion

A novel series of phenoxymethybenzoimidazole incorporating different aryl thiazole-triazole acetamide derivatives (**9a-n**) were rationally designed, synthesized, and evaluated for their α-glycosidase inhibitory activity. All tested derivatives demonstrated better α-glucosidase inhibitory potential with an IC_{50} value ranging from 6.31 to 49.89 µM compared

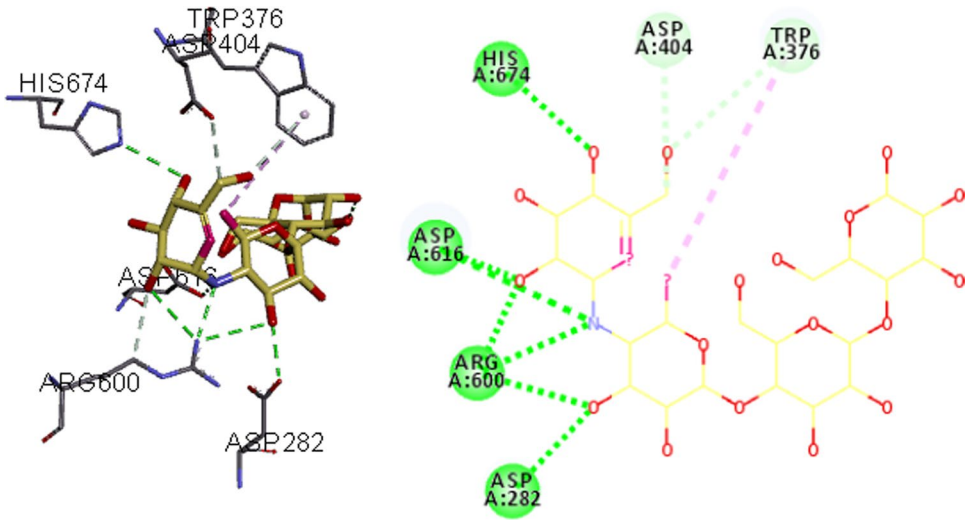

Fig. 4 The 3D and 2D in traction of the top-scoring pose of acarbose within the α-glycosidase active site

Table 2 Docking scores and interactions of **9c**, **9g**, **9m** compounds against the α-glycosidase

Compound	Gold score	Category (type)	Ligand involved moiety	Receptor involved part
9c	66.30	Hydrogen Bond	NH of benzimidazole	Asp616
		Pi-Pi-Stacked	Benzimidazole	Phe649
		Pi-Pi-Stacked	Benzimidazole	Phe649
		Pi-Anion	Benzimidazole	Asp518
		Pi-Anion	Benzimidazole	Asp518
		Pi-Cation	Benzimidazole	Arg600
		Pi-Alkyl	Benzimidazole	Met519
		Pi-Sulfur	Phenoxymethyl	Met519
		Pi-Anion	Phenoxymethyl	Asp282
		Van der Waals	Phenoxymethyl	Asp282
		Hydrogen Bond	Triazole	Ala284
		Pi-Alkyl	Triazole	Ala284
		Van der Waals	Triazole	Leu283
		Pi-Alkyl	Triazole	Leu283
		Pi-Sigma	Thiazole	Leu650
		Amide-Pi-Stacked	Bromophenyl	Gly651
		Pi-Alkyl	Bromophenyl	Leu678
		Pi-Alkyl	Bromophenyl	Leu678
9 g	70.16	Hydrogen Bond	NH of benzimidazole	Asp616
		Pi-Pi-Stacked	Benzimidazole	Phe649
		Pi-Anion	Benzimidazole	Asp518
		Pi-Anion	Benzimidazole	Asp518
		Pi-Cation	Benzimidazole	Arg600
		Pi-Sulfur	Methoxyphenoxymethyl	Arg600
		Pi-Anion	Methoxyphenoxymethyl	Asp282
		Hydrogen Bond	Methoxyphenoxymethyl	Asp616
		Hydrogen Bond	Methoxyphenoxymethyl	Asp282
		Van der Waals	Triazole	Arg281
		Pi-Alkyl	Triazole	Leu283
		Hydrogen Bond	Acetamide	Ala284
		Pi-Sulfur	Thiazole	Trp618
		Pi-Alkyl	Thiazole	Leu283
		Pi- Sigma	Thiazole	Ala284
		Hydrogen Bond	Thiazole	Ala284

Table 2 (continued)

Compound	Gold score	Category (type)	Ligand involved moiety	Receptor involved part
9 m	68.53	Hydrogen Bond	NH of benzimidazole	Asn524
		Hydrogen Bond	N of benzimidazole	Arg281
		Alkyl- Alkyl	Methyl Benzimidazole	Ala554
		Pi-Alkyl	Benzimidazole	Ala554
		Pi-Alkyl	Benzimidazole	Arg527
		Pi-Alkyl	Benzimidazole	Ala555
		Pi- Sigma	Benzimidazole	Ala555
		Pi-Alkyl	Phenoxymethyl	Ala555
		Hydrogen Bond	Triazole	Arg600
		Pi-Alkyl	Triazole	Met519
		Sulfur –Alkyl	Triazole	Met519
		Sulfur –Alkyl	Triazole	Met519
		Pi-Pi T-shaped	Triazole	Trp481
		Pi-Anion	Triazole	Asp616
		Pi-Anion	Thiazole	Phe649
		Pi-Sigma	Methylphenyl	Leu650
		Pi-Alkyl	Methylphenyl	Tro618
		Pi-Alkyl	Methylphenyl	Leu678

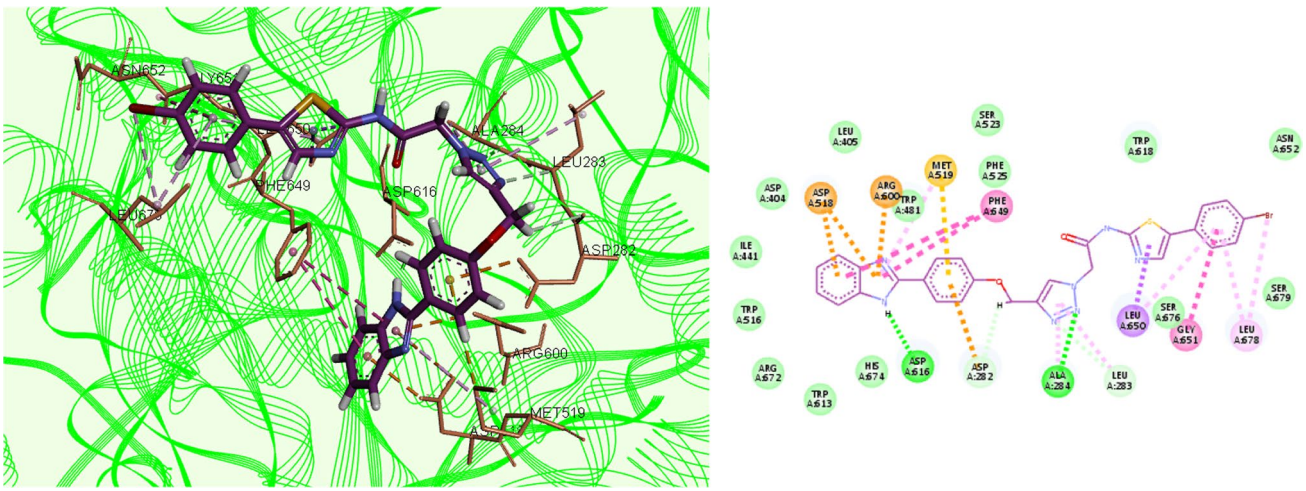

Fig. 5. 3D and 2D interaction patterns of compounds **9c** in the active site of α-glycosidase

to standard drug acarbose ($IC_{50} = 750.0 \pm 10.0$ µM). Among the series, compound **9g** ($IC_{50} = 6.31$ µM; $R^1 = H$, $R^2 = H$, $R^3 = OCH_3$), **9m** ($IC_{50} = 8.30$ µM; $R^1 = 4CH_3$, $R^2 = CH_3$, $R^3 = H$), and **9c** ($IC_{50} = 8.88$ µM; $R^1 = 4Br$, $R^2 = H$, $R^3 = H$) were found to be the most potent α-glycosidase inhibitors. According to SAR analysis, it was found that the phenoxymethybenzoimidazole bearing thiazole-triazole acetamide as the basic skeleton of compounds was responsible for this promising α-glycosidase inhibition. The obtained SAR profile found that in the case of benzoimidazole core (**9a-j**), $2OCH_3$-substituted on phenoxy (R^3), while $R^1 = H$ contributed to the improved inhibitory activity. Additionally, in the other set bearing methyl-benzoimidazole (**9k-n**) small and moderate electron-donating group at R^1 is more favorable.

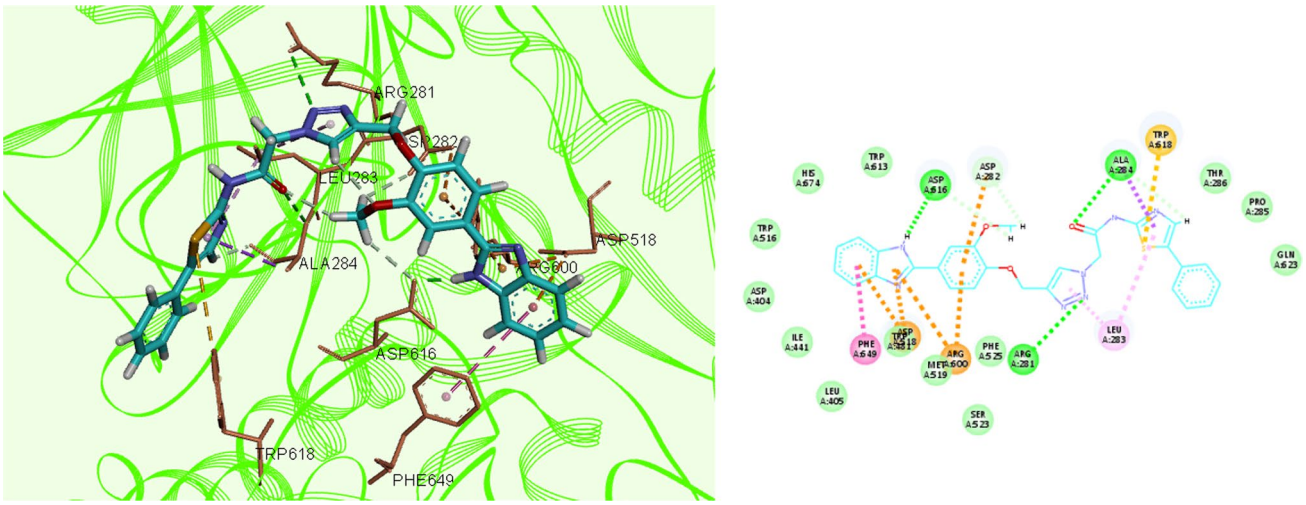

Fig. 6. 3D and 2D interaction patterns of compounds **9g** in the active site of α-glycosidase

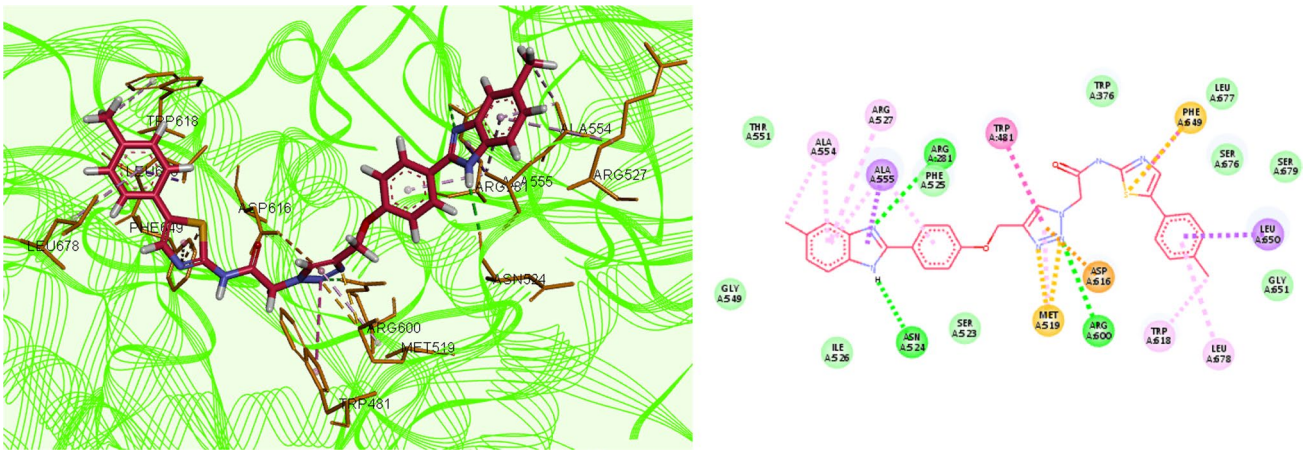

Fig. 7. 3D and 2D interaction patterns of compounds **9m** in the active site of α-glycosidase

The in vitro kinetic assay of **9g**, **9m,** and **9c** presented the uncompetitive type of inhibition against α-glycosidase. Docking studies showed the critical role of benzoimidazole and triazole moieties of the synthesized compounds to fit properly into the active site and occupy the binding site of α-glycosidase. Even though the inhibitory activities of compounds **9g**, **9m**, and **9c** were considered quite good, due to the presence of benzoimidazole and phenoxymethyltriazole moieties which effectively participated in interactions with the critical residues of the α-glycosidase active site, the important role of aryl-substituted at R^1 should not be neglected. The substituted groups at R^1 rather than providing additional hydrophobic interactions, played the dominant role in the conformation of these derivatives in the α-glycosidase active site.

Experimental section

Chemistry

All reagents of this protocol were purchased from chemical suppliers and used without further purification. The purity of synthesized analogs was checked through TLC (aluminum plates precoated with silica gel, Kieselgel 60, 254, E. Merck, Germany). The melting points of 9a-n were determined on a Kofler hot stage apparatus. Nicolet Magna FTIR 550 spectrophotometer was used to record IR spectra of the synthesized compounds by using KBr disks. ^{1}H-NMR and ^{13}C-NMR were carried out on Avance Bruker 500 MHz.

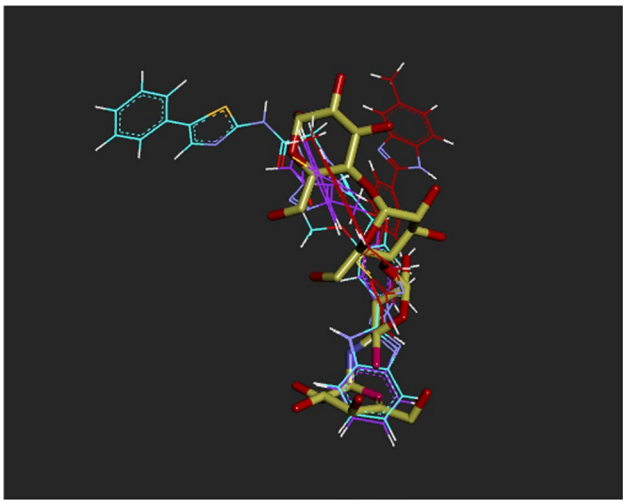

Fig. 8 Representation of the docking poses of compounds over the active site. Acarbose was presented in yellow in stick mode, while **9c**, **9g**, and **9m** were shown in purple, cyan, and red color in line mode

2-(4-(Prop-2-yn-1-yloxy)phenyl)-1H-benzo[d]imidazole (8a)

In a round-bottom flask, 10 mmol benzene-1,2-diamine (**6a**) and 10 mmol 4-(prop-2-yn-1-yloxy)benzaldehyde (**7a**) were dissolved in DMF in the presence of $Na_2S_2O_5$. The reaction mixture was then stirred at 100 °C for 4 h and then the crude product was extracted and recrystallized in EtOH. ^{1}H NMR (400 MHz,DMSO-d_6) δ 9.9 (s, 1H, NH), 8.17 (d, *J* = *8.9 Hz*, 2H, H 2,6 Ph),7.67–7.62 (m, 2H, H 4,7), 7.28–7.24 (m, 2H, H 5,6), 7.86 (m, 1H, H-6), 7.20 (d, *J* = 8.9 Hz, 2H, H3,5 Ph), 4.92 (s, 2H,CH_2), 3.65 (s, 1H,CH).

2-{4-[4-(1H-1,3-benzodiazol-2-yl)phenoxymethyl]-1H-1,2,3-triazol-1-yl}-N-(2-phenyl-1,3-thiazol-5-yl)acetamide (9a)

White solid; isolated yield: 89%; mp 170–172 °C; IR (KBr, υ): 3354, 2921, 1673 cm^{-1}; ^{1}H NMR (400 MHz, DMSO-d_6) δ 13.04–12.82 (m, 2H, 2 × NH), 8.42 (s, 1H), 8.21 (d, *J* = 8.3 Hz, 2H), 7.94 – 7.89 (m, 2H), 7.81 (s, 1H), 7.71–7.68 (m, 2H), 7.65–7.61 (m, 1H), 7.35–7.18 (m, 6H), 5.62 (s, 2H, H-23), 5.36 (s, 2H, H-17); ^{13}C NMR (101 MHz, DMSO-d_6) δ 164.99, 162.26, 159.36, 159.24, 158.87, 157.50, 147.78, 143.03, 142.38, 133.25, 131.69, 127.98, 127.66, 126.49, 123.10, 122.99, 120.97, 115.30, 115.10, 115.06, 109.37, 61.10 (C-17), 51.48 (C-23); Anal Calcd for $C_{27}H_{21}N_7O_2S$: C, 63.89; H, 4.17; N, 19.32; found: C, 63.86; H, 4.20; N, 19.37.

2-{4-[4-(1H-1,3-benzodiazol-2-yl)phenoxymethyl]-1H-1,2,3-triazol-1-yl}-N-[2-(4-fluorophenyl)-1,3-thiazol-5-yl] acetamide (9b)

White solid; isolated yield: 82%; mp 192–194 °C; IR (KBr, υ): 3351, 2928, 1682 cm^{-1}; ^{1}H NMR (400 MHz, DMSO-d_6) δ 12.86 (s, 1H, NH), 12.74–12.68 (m, 1H), 8.39 (s, 1H), 8.16 (d, *J* = 8.3 Hz, 2H), 8.00 (dd, *J* = 8.7, 5.6 Hz, 2H), 7.72 (s, 1H), 7.67 (d, *J* = 8.7 Hz, 1H), 7.56–7.53 (m, 1H), 7.46–7.40 (m, 1H), 7.34–7.28 (m, 4H), 7.06–7.02 (m, 1H), 5.59 (s, 2H, H-23), 5.33 (s, 2H, H-17); ^{13}C NMR (101 MHz, DMSO-d_6) δ 164.42 (d, *J* = 252.1 Hz), 160.55, 159.35, 157.64, 147.90, 142.33, 130.73, 127.96, 127.81, 127.62, 126.48, 122.94, 121.42, 118.48, 118.07, 115.73, 115.52, 115.25, 115.04, 111.03, 110.80, 110.54, 108.29, 61.06 (C-17), 51.53 (C-23); Anal Calcd for $C_{27}H_{20}FN_7O_2S$: C, 61.70; H, 3.84; N, 18.66; found: C, 61.77; H, 3.80; N, 18.65.

2-{4-[4-(1H-1,3-benzodiazol-2-yl)phenoxymethyl]-1H-1,2,3-triazol-1-yl}-N-[2-(4-bromophenyl)-1,3-thiazol-5-yl] acetamide (9c)

White solid; isolated yield: 92%; mp 212–214 °C; IR (KBr, υ): 3351, 2925, 1678 cm^{-1}; ^{1}H NMR (400 MHz, DMSO-d_6) δ 13.24–12.33 (m, 2H, 2 × NH), 8.43 (s, 1H), 8.22 (d, *J* = 8.1 Hz, 2H), 7.98 (d, *J* = 7.2 Hz, 1H), 7.75 (s, 1H), 7.66–7.63 (m, 2H), 7.50 (t, *J* = 7.5 Hz, 2H), 7.42–7.38 (m, 1H), 7.32 (d, *J* = 8.2 Hz, 2H), 7.25–7.23 (m, 2H), 5.63 (s, 2H, H-23), 5.36 (s, 2H, H-17); ^{13}C NMR (101 MHz, DMSO-d_6) δ 164.92, 162.26, 159.40, 159.31, 159.27, 158.89, 157.29, 148.97, 142.36, 137.91, 134.04, 128.76, 128.01, 127.89, 126.50, 125.64, 122.99, 122.89, 121.81, 115.11, 115.07, 61.09 (C-17), 51.48 (C-23); Anal Calcd for $C_{27}H_{20}BrN_7O_2S$: C, 55.30; H, 3.44; N, 16.72; found: C, 55.26; H, 3.46; N, 16.76.

2-{4-[4-(1H-1,3-benzodiazol-2-yl)phenoxymethyl]-1H-1,2,3-triazol-1-yl}-N-[2-(4-methylphenyl)-1,3-thiazol-5-yl]acetamide(9d)

White solid; isolated yield: 90%; mp 197–199 °C; IR (KBr, υ): 3353, 2925, 1679 cm^{-1}; ^{1}H NMR (400 MHz, DMSO-d_6) δ 12.91 (s, 1H, NH), 8.42 (s, 1H), 8.30–8.15 (m, 2H), 7.85 (d, *J* = 8.1 Hz, 2H), 7.68–7.58 (m, 3H), 7.35–7.16 (m, 7H), 5.61 (s, 2H, H-23), 5.35 (s, 2H, H-17), 2.36 (s, 3H, CH_3); ^{13}C NMR (101 MHz, DMSO-d_6) δ 164.84, 159.44, 157.18, 151.61, 151.47, 149.07, 142.38, 139.50, 139.08, 137.22, 131.40, 129.30, 128.02, 126.50, 125.59, 122.85, 121.87, 115.09, 114.76, 114.66, 107.65, 61.12 (C-17), 51.49 (C-23), 20.77 (CH3); Anal Calcd for $C_{28}H_{23}N_7O_2S$: C, 64.48; H, 4.44; N, 18.80; found: C, 64.44; H, 4.50; N, 18.87.

2-{4-[4-(1H-1,3-benzodiazol-2-yl)phenoxymethyl]-1H-1,2,3-triazol-1-yl}-N-[2-(4-methoxyphenyl)-1,3-thiazol-5-yl]acetamide (9e)

White solid; isolated yield: 87%; mp 245–247 °C; IR (KBr, υ): 3356, 2921, 1680 cm^{-1}; ^{1}H NMR (400 MHz, DMSO-d_6) δ 12.95–12.87 (m, 2H, 2 × NH), 8.46 (s, 1H), 8.24 (d, *J* = 8.6 Hz, 2H), 7.94 (d, *J* = 8.8 Hz, 1H), 7.83–7.47 (m, 4H), 7.35 (d, *J* = 8.6 Hz, 2H), 7.30–7.26 (m, 2H), 7.10 (d, *J* = 8.9 Hz, 2H), 5.64 (s, 2H, H-23), 5.39 (s, 2H, H-17), 3.89 (s, 3H, OCH_3); ^{13}C NMR (101 MHz, DMSO-d_6) δ 164.81, 162.26, 159.36, 159.00, 157.31, 157.13, 155.01, 151.25, 148.85, 147.26, 142.35, 130.05, 127.97, 126.99,

126.87, 126.49, 126.21, 122.96, 115.05, 114.09, 106.50, 61.08 (C-17), 55.11 (OCH3), 51.46 (C-23); Anal Calcd for $C_{28}H_{23}N_7O_3S$: C, 62.56; H, 4.31; N, 18.24; found: C, 62.50; H, 4.32; N, 18.28.

2-{4-[4-(1H-1,3-benzodiazol-2-yl)phenoxymethyl]-1H-1,2,3-triazol-1-yl}-N-[2-(3-methoxyphenyl)-1,3-thiazol-5-yl]acetamide (9f)

White solid; isolated yield: 95%; mp 182–184 °C; IR (KBr, υ): 3357, 2924, 1670 cm^{-1}; ^1H NMR (400 MHz, DMSO-d_6) δ 13.03–12.70 (m, 2H, 2 × NH), 8.41 (s, 1H), 8.20 (d, $J = 8.2$ Hz, 2H), 7.77 (s, 1H), 7.69–7.58 (m, 2H), 7.57–7.49 (m, 2H), 7.40 (t, $J = 7.8$ Hz, 1H), 7.31 (d, $J = 8.0$ Hz, 2H), 7.25–7.19 (m, 2H), 6.96 (d, $J = 8.0$ Hz, 1H), 5.60 (s, 2H, H-23), 5.35 (s, 2H, H-17), 3.86 (s, 3H, OCH_3); ^{13}C NMR (101 MHz, DMSO-d_6) δ 164.92, 162.04, 159.57, 159.37, 157.18, 151.33, 148.81, 143.90, 142.38, 139.99, 138.22, 135.41, 132.40, 129.84, 127.98, 126.49, 122.97, 121.77, 118.02, 115.06, 113.68, 110.88, 108.94, 61.10 (C-17), 55.06 (OCH3), 51.47 (C-23); Anal Calcd for $C_{28}H_{23}N_7O_3S$: C, 62.56; H, 4.31; N, 18.24; found: C, 62.55; H, 4.35; N, 18.28.

2-{4-[4-(1H-1,3-benzodiazol-2-yl)-2-methoxyphenoxymethyl]-1H-1,2,3-triazol-1-yl}-N-(2-phenyl-1,3-thiazol-5-yl)acetamide (9g)

White solid; isolated yield: 91%; mp 238–240 °C; IR (KBr, υ): 3357, 2926, 1683 cm^{-1}; ^1H NMR (400 MHz, DMSO-d_6) δ 13.31–12.51 (m, 2H, 2 × NH), 8.39 (s, 1H), 7.96–7.92 (m, 2H), 7.87–7.81 (m, 2H), 7.69 (s, 1H), 7.63–7.59 (m, 2H), 7.45 (t, $J = 7.7$ Hz, 2H), 7.40–7.33 (m, 2H), 7.22–7.18 (m, 2H), 5.60 (s, 2H, H-23), 5.29 (s, 2H, H-17), 3.91 (s, 3H, OCH_3); ^{13}C NMR (101 MHz, DMSO-d_6) δ 164.96, 162.26, 157.30, 151.40, 151.30, 149.04, 148.97, 148.91, 142.36, 139.41, 137.33, 134.04, 128.75, 127.89, 126.63, 125.64, 123.15, 121.79, 119.11, 113.38, 113.17, 109.84, 108.54, 61.48 (C-17), 55.49 (OCH3), 51.49 (C-23); Anal Calcd for $C_{28}H_{23}N_7O_3S$: C, 62.56; H, 4.31; N, 18.24; found: C, 62.55; H, 4.36; N, 18.20.

2-{4-[4-(1H-1,3-benzodiazol-2-yl)-2-methoxyphenoxymethyl]-1H-1,2,3-triazol-1-yl}-N-[2-(4-bromophenyl)-1,3-thiazol-5-yl]acetamide (9h)

White solid; isolated yield: 84%; mp 200–202 °C; IR (KBr, υ): 3359, 2926, 1675 cm^{-1}; ^1H NMR (400 MHz, DMSO-d_6) δ 13.26–12.62 (m, 2H, 2 × NH), 8.43 (s, 1H), 7.93–7.86 (m, 4H), 7.75 (s, 1H), 7.66 (d, $J = 8.2$ Hz, 4H), 7.42 (d, $J = 8.3$ Hz, 1H), 7.25–7.22 (m, 2H), 5.64 (s, 2H, H-23), 5.33 (s, 2H, H-17), 3.94 (s, 3H, OCH_3); ^{13}C NMR (101 MHz, DMSO) δ 165.07, 162.25, 157.65, 151.45, 149.06, 148.93, 148.90, 148.81, 147.79, 142.39, 133.26, 131.65, 127.63, 126.62, 123.34, 123.18, 123.18, 121.79, 120.97, 119.13, 113.17, 109.84, 109.26, 61.50 (C-17), 55.47 (OCH3), 51.55 (C-23); Anal Calcd for $C_{28}H_{22}BrN_7O_3S$: C, 54.55; H, 3.60; N, 15.90; found: C, 54.50; H, 3.67; N, 15.93.

2-{4-[4-(1H-1,3-benzodiazol-2-yl)-2-methoxyphenoxymethyl]-1H-1,2,3-triazol-1-yl}-N-[2-(4-methylphenyl)-1,3-thiazol-5-yl]acetamide (9i)

White solid; isolated yield: 94%; mp 227–229 °C; IR (KBr, υ): 3355, 2930, 1691 cm^{-1}; ^1H NMR (400 MHz, DMSO-d_6) δ 13.05–12.81 (m, 1H, NH), 8.42 (s, 1H), 7.92–7.83 (m, 4H), 7.67–7.62 (m, 3H), 7.42 (d, $J = 8.5$ Hz, 1H), 7.34–7.16 (m, 5H), 5.63 (s, 2H, H-23), 5.33 (s, 2H, H-17), 3.95 (s, 3H, OCH_3), 2.36 (s, 3H, CH_3); ^{13}C NMR (101 MHz, DMSO-d_6) δ 164.89, 162.26, 157.18, 153.72, 151.29, 149.06, 149.05, 149.03, 145.83, 142.34, 139.00, 137.21, 131.39, 129.30, 126.64, 125.59, 122.81, 121.96, 119.23, 114.70, 113.16, 109.90, 107.64, 61.48 (C-17), 55.51 (OCH3), 51.48 (C-23), 20.77 (CH3); Anal Calcd for $C_{29}H_{25}N_7O_3S$: C, 63.14; H, 4.57; N, 17.77; found: C, 63.15; H, 4.55; N, 17.80.

2-{4-[4-(1H-1,3-benzodiazol-2-yl)-2-methoxyphenoxymethyl]-1H-1,2,3-triazol-1-yl}-N-[2-(4-methoxyphenyl)-1,3-thiazol-5-yl]acetamide (9j)

White solid; isolated yield: 95%; mp 196–198 °C; IR (KBr, υ): 3352, 2926, 1673 cm^{-1}; ^1H NMR (400 MHz, DMSO-d_6) δ 12.98–12.77 (m, 2H, 2 × NH), 8.41 (s, 1H), 7.93–7.78 (m, 5H), 7.65–7.60 (m, 1H), 7.55 (s, 1H), 7.42 (d, $J = 8.5$ Hz, 1H), 7.25–7.22 (m, 2H), 7.05 (d, $J = 8.9$ Hz, 2H), 5.61 (s, 2H, H-23), 5.32 (s, 2H, H-17), 3.94 (s, 3H, OCH_3), 3.83 (s, 3H, OCH_3); ^{13}C NMR (101 MHz, DMSO-d_6) δ 164.96, 162.26, 157.30, 151.40, 149.04, 148.97, 148.91, 142.36, 139.41, 137.33, 134.04, 128.75, 127.89, 126.63, 125.64, 123.15, 121.79, 119.11, 113.38, 113.17, 109.84, 108.54, 61.48, 55.49, 51.49; ^{13}C NMR (101 MHz, DMSO) δ 164.83, 162.26, 159.00, 157.15, 151.39, 149.03, 148.91, 148.86, 148.79, 142.35, 126.99, 126.88, 126.61, 126.20, 123.31, 123.14, 119.06, 114.08, 113.37, 113.16, 110.14, 109.77, 106.48, 61.47 (C-17), 55.46 (OCH3), 55.10 (OCH3), 51.47 (C-23); Anal Calcd for $C_{29}H_{25}N_7O_4S$: C, 61.36; H, 4.44; N, 17.27; found: C, 61.40; H, 4.50; N, 17.20.

2-{4-[4-(6-Methyl-1H-1,3-benzodiazol-2-yl)phenoxymethyl]-1H-1,2,3-triazol-1-yl}-N-(2-phenyl-1,3-thiazol-5-yl)acetamide (9k)

White solid; isolated yield: 87%; mp 172–174 °C; IR (KBr, υ): 3355, 2928, 1695 cm^{-1}; ^1H NMR (400 MHz, DMSO-d_6) δ 12.93 (s, 1H, NH), 12.82–12.54 (m, 1H, NH), 8.41 (s, 1H), 8.18 (d, $J = 8.3$ Hz, 2H), 7.97 (d, $J = 7.3$ Hz, 2H), 7.73 (s, 1H), 7.54–7.47 (m, 3H), 7.43–7.34 (m, 2H), 7.30 (d, $J = 8.5$ Hz, 2H), 7.05 (d, $J = 8.1$ Hz, 1H), 5.61 (s, 2H, H-23), 5.35 (s, 2H, H-17), 2.47 (s, 3H, CH_3); ^{13}C NMR (101 MHz, DMSO-d_6) δ 164.92, 159.23, 157.30, 153.73, 148.96, 145.60, 142.38, 137.46, 135.87, 134.04, 130.87, 128.76, 127.89, 127.84, 126.49, 125.64, 123.14, 119.51, 115.01, 110.88, 108.55, 61.08 (C-17), 51.48 (C-23), 21.31 (CH3); Anal Calcd for $C_{28}H_{23}N_7O_2S$: C, 64.48; H, 4.44; N, 18.80; found: C, 64.44; H, 4.45; N, 18.86.

N-[2-(4-bromophenyl)-1,3-thiazol-5-yl]-2-{4-[4-(6-methyl-1H-1,3-benzodiazol-2-yl) phenoxymethyl]-1H-1,2,3-triazol-1-yl}acetamide (9l)

White solid; isolated yield: 89%; mp 194–196 °C; IR (KBr, υ): 3351, 2917, 1688 cm^{-1}; ^{1}H NMR (400 MHz, DMSO-d_6) δ 13.20–12.76 (m, 1H, NH), 12.71 (s, 1H, NH), 8.18–8.16 (m, 2H), 7.91 (d, J = 8.6 Hz, 2H), 7.81 (s, 1H), 7.69 (d, J = 8.6 Hz, 2H), 7.56–7.53 (m, 1H), 7.47–7.41 (m, 2H), 7.33 (s, 1H), 7.06–7.02 (m, 2H), 5.59 (s, 2H, H-23), 5.33 (s, 2H, H-17), 2.55 (s, 3H, CH_3); ^{13}C NMR (101 MHz, DMSO-d_6) δ 165.05, 159.07, 158.70, 157.60, 147.74, 143.03, 142.35, 137.92, 133.27, 131.69, 127.83, 127.66, 126.48, 122.99, 120.94, 118.30, 118.07, 115.24, 115.00, 110.81, 109.36, 61.06 (C-17), 51.50 (C-23), 21.31 (CH3); Anal Calcd for $C_{28}H_{22}BrN_7O_2S$: C, 56.00; H, 3.69; N, 16.33; found: C, 56.07; H, 3.67; N, 16.38.

2-{4-[4-(6-Methyl-1H-1,3-benzodiazol-2-yl) phenoxymethyl]-1H-1,2,3-triazol-1-yl}-N-[2-(4-methylphenyl)-1,3-thiazol-5-yl]acetamide (9m)

White solid; isolated yield: 90%; mp 208–210 °C; IR (KBr, υ): 3351, 2924, 1693 cm^{-1}; ^{1}H NMR (400 MHz, DMSO-d_6) δ 12.87 (s, 1H, NH), 12.68 (s, 1H), 8.40 (s, 1H), 8.16 (d, J = 8.5 Hz, 3H), 7.89 (d, J = 8.8 Hz, 2H), 7.57 (s, 1H), 7.48–7.43 (m, 1H), 7.29 (d, J = 8.8 Hz, 2H), 7.06–7.04 (m, 3H), 5.59 (s, 2H, H-23), 5.33 (s, 2H, H-17), 2.50–2.43 (m, 6H, 2 × CH_3); ^{13}C NMR (101 MHz, DMSO-d_6) δ 164.81, 159.21, 159.00, 158.72, 157.13, 150.87, 148.84, 143.03, 142.35, 137.92, 127.82, 126.98, 126.87, 126.48, 123.12, 122.98, 115.25, 115.01, 114.09, 110.54, 106.50, 61.06 (C-17), 51.45 (C-23), 21.81 (CH3), 21.31 (CH3); Anal Calcd for $C_{29}H_{25}N_7O_2S$: C, 65.03; H, 4.70; N, 18.31; found: C, 65.08; H, 4.69; N, 18.33.

N-[2-(4-methoxyphenyl)-1,3-thiazol-5-yl]-2-{4-[4-(6-methyl-1H-1,3-benzodiazol-2-yl) phenoxymethyl]-1H-1,2,3-triazol-1-yl}acetamide (9n)

White solid; isolated yield: 87%; mp 197–199 °C; IR (KBr, υ): 3352, 2928, 1683 cm^{-1}; ^{1}H NMR (400 MHz, DMSO-d_6) δ 12.87 (s, 1H, NH), 12.79–12.52 (m, 1H), 8.40 (s, 1H), 8.16 (d, J = 7.9 Hz, 2H), 7.89 (d, J = 8.8 Hz, 2H), 7.57 (s, 1H), 7.52–7.43 (m, 1H), 7.42–7.34 (m, 1H), 7.29 (d, J = 8.3 Hz, 2H), 7.07–7.03 (m, 3H), 5.58 (s, 2H, H-23), 5.33 (s, 2H, H-17), 3.84 (s, 3H, OCH_3), 2.47 (s, 3H, CH_3); ^{13}C NMR (101 MHz, DMSO-d_6) δ 164.80, 159.22, 159.01, 157.12, 148.84, 146.30, 142.36, 138.65, 137.62, 133.75, 132.79, 127.82, 126.98, 126.88, 126.47, 123.12, 118.58, 115.01, 114.09, 109.69, 106.51, 61.07 (C-17), 55.12 (OCH3), 51.45 (C-23), 21.31 (CH3); Anal Calcd for $C_{29}H_{25}N_7O_3S$: C, 63.14; H, 4.57; N, 17.77; found: C, 63.18; H, 4.50; N, 17.79.

α-Glycosidase inhibition assay

The anti-α-glycosidase effects of synthesized compound **9a-n** were screened according to the previously reported method. Briefly, 135 µL of potassium phosphate buffer, 20 µL of target compounds **9a-n** with various concentrations, and 20 µL of α-glycosidase solution were added to each well in the 96-well plate and incubated for 10 min at 37 °C. Then, *p*-nitrophenyl glucopyranoside as substrate (25 µL, 4 mM) was added and incubation was continued at 37 °C for 20 min. Finally, absorbance was measured at 405 nm by a spectrophotometer [37–41].

Enzyme kinetic study

The mode of inhibition of the most active compound (**9c**, **9g**, and **9m**), identified with the lowest IC_{50}, was investigated against an α-glycosidase activity with different concentrations of *p*-nitrophenyl *α*-D-glucopyranoside (2–10 mM) as substrate in the absence and presence of sample (**9c**, **9g**, and **9m**) at different concentrations (0, 1.25, 2.5, 5, and 10 µM). A Lineweaver–Burk plot was generated to identify the type of inhibition, and the Michaelis–Menten constant ($1/V'_{max}$) value was determined from the plot between reciprocal of the substrate concentration (1/[S]) and reciprocal of enzyme rate (1/V) over various inhibitor concentrations. The experimental inhibitor constant (K_i) value was constructed by secondary plots of the inhibitor concentration [I] versus $1/Vi'_{max}$ [15, 42, 43].

Molecular docking

The 3D structure of α-glycosidase (PDB entry code: 5NN8) in complex with acarbose was obtained from the protein data bank. After editing the crystallographic structure which contains removing ligand and water molecules and adding hydrogen atoms, the prepared ligands (the ligands were sketched in HyperChem software and energy minimized by the MM1 force field) were docked into the active site of the enzyme. The binding site of the enzyme for the docking was defined automatically using the coordinates of the native ligand acarbose in such a way that 10 Å around the ligand was defined as the binding site. Gold docking program with ChemScore function was used for docking analyses and re-dock acarbose inside the 5NN8. The top-score binding poses were used for further analysis. Protein–ligand interactions were analyzed with Discovery Studio Visualizer [17].

Supplementary Information The online version contains supplementary material available at https://doi.org/10.1007/s11030-021-10310-7.

Declarations

Conflict of interest The authors declare that they have no known competing financial interests or personal relationships that could have appeared to influence the work reported in this paper.

References

1. Wondafrash DZ, Desalegn TZ, Yimer EM, Tsige AG, Adamu BA, Zewdie KA (2020) Potential effect of hydroxychloroquine in diabetes mellitus: a systematic review on preclinical and clinical trial studies. J Diabetes Res 2020:5214751. https://doi.org/10.1155/2020/5214751
2. Carvalho DS, de Almeida AA, Borges AF, Vannucci Campos D (2018) Treatments for diabetes mellitus type II: new perspectives regarding the possible role of calcium and cAMP interaction. Eur J Pharmacol 830:9–16. https://doi.org/10.1016/j.ejphar.2018.04.002
3. Katsarou A, Gudbjörnsdottir S, Rawshani A, Dabelea D, Bonifacio E, Anderson BJ, Jacobsen LM, Schatz DA, Lernmark Å (2017) Type 1 diabetes mellitus. Nat Rev Dis Primers 3(1):1–17
4. Khursheed R, Singh SK, Wadhwa S, Kapoor B, Gulati M, Kumar R, Ramanunny AK, Awasthi A, Dua K (2019) Treatment strategies against diabetes: Success so far and challenges ahead. Eur J Pharmacol 862:172625. https://doi.org/10.1016/j.ejphar.2019.172625
5. Anthony S, Odgers T, Kelly W (2004) Health promotion and health education about diabetes mellitus. R Soc Health J 124(2):70–73
6. Ogawa S, Nako K, Okamura M, Sakamoto T, Ito S (2015) Stabilization of postprandial blood glucose fluctuations by addition of glucagon like polypeptide-analog administration to intensive insulin therapy. J Diabetes Investig 6(4):436–442
7. Xiao J, Hogger P (2015) Dietary polyphenols and type 2 diabetes: current insights and future perspectives. Curr Med Chem 22(1):23–38
8. Tundis R, Loizzo M, Menichini F (2010) Natural products as α-amylase and α-glucosidase inhibitors and their hypoglycaemic potential in the treatment of diabetes: an update. Mini Rev Med Chem 10(4):315–331
9. Pedrood K, Sherafati M, Mohammadi-Khanaposhtani M, Asgari MS, Hosseini S, Rastegar H, Larijani B, Mahdavi M, Taslimi P, Erden Y (2021) Design, synthesis, characterization, enzymatic inhibition evaluations, and docking study of novel quinazolinone derivatives. Int J Biol Macromol 170:1–12
10. Gulçin İ, Taslimi P, Aygün A, Sadeghian N, Bastem E, Kufrevioglu OI, Turkan F, Şen F (2018) Antidiabetic and antiparasitic potentials: inhibition effects of some natural antioxidant compounds on α-glycosidase, α-amylase and human glutathione S-transferase enzymes. Int J Biol Macromol 119:741–746. https://doi.org/10.1016/j.ijbiomac.2018.08.001
11. Hakamata W, Kurihara M, Okuda H, Nishio T, Oku T (2009) Design and screening strategies for α-glucosidase inhibitors based on enzymological information. Curr Top Med Chem 9(1):3–12
12. Menteşe E, Baltaş N, Bekircan O (2019) Synthesis and kinetics studies of N′-(2-(3,5-disubstituted-4H-1,2,4-triazol-4-yl) acetyl)-6/7/8-substituted-2-oxo-2H-chromen-3-carbohydrazide derivatives as potent antidiabetic agents. Arch Pharm 352(12):1900227. https://doi.org/10.1002/ardp.201900227
13. Yin Z, Zhang W, Feng F, Zhang Y, Kang W (2014) α-Glucosidase inhibitors isolated from medicinal plants. Food Sci Hum Well 3(3–4):136–174
14. Chaudhry F, Shahid W, Al-Rashida M, Ashraf M, Munawar MA, Khan MA (2021) Synthesis of imidazole-pyrazole conjugates bearing aryl spacer and exploring their enzyme inhibition potentials. Bioorg Chem 108:104686
15. Azimi F, Ghasemi JB, Azizian H, Najafi M, Faramarzi MA, Saghaei L, Sadeghi-Aliabadi H, Larijani B, Hassanzadeh F, Mahdavi M (2021) Design and synthesis of novel pyrazole-phenyl semicarbazone derivatives as potential α-glucosidase inhibitor: kinetics and molecular dynamics simulation study. Int J Biol Macromol 166:1082–1095
16. Sherafati M, Mirzazadeh R, Barzegari E, Mohammadi-Khanaposhtani M, Azizian H, Sadegh Asgari M, Hosseini S, Zabihi E, Mojtabavi S, Ali Faramarzi M, Mahdavi M, Larijani B, Rastegar H, Hamedifar H, Hamed Hajimiri M (2021) Quinazolinone-dihydropyrano[3,2-b]pyran hybrids as new α-glucosidase inhibitors: design, synthesis, enzymatic inhibition, docking study and prediction of pharmacokinetic. Bioorg Chem 109:104703. https://doi.org/10.1016/j.bioorg.2021.104703
17. Shareghi-Boroujeni D, Iraji A, Mojtabavi S, Faramarzi MA, Akbarzadeh T, Saeedi M (2021) Synthesis, in vitro evaluation, and molecular docking studies of novel hydrazineylideneindolinone linked to phenoxymethyl-1,2,3-triazole derivatives as potential α-glucosidase inhibitors. Bioorg Chem 111:104869. https://doi.org/10.1016/j.bioorg.2021.104869
18. Zarenezhad E, Farjam M, Iraji A (2021) Synthesis and biological activity of pyrimidines-containing hybrids: focusing on pharmacological application. J Mol Struct 1230:129833. https://doi.org/10.1016/j.molstruc.2020.129833
19. Santos CMM, Freitas M, Fernandes E (2018) A comprehensive review on xanthone derivatives as α-glucosidase inhibitors. Eur J Med Chem 157:1460–1479. https://doi.org/10.1016/j.ejmech.2018.07.073
20. Sari S, Barut B, Özel A, Saraç S (2020) Discovery of potent α-glucosidase inhibitors through structure-based virtual screening of an in-house azole collection. Chem Biol Drug Des 97:701–710
21. Hbb AG (1994) Pharmacology of α-glucosidase inhibition. Eur J Clin Invest 24(S3):3–10
22. Scott LJ, Spencer CM (2000) Miglitol. Drugs 59(3):521–549
23. Kumar S, Sharma B, Mehra V, Kumar V (2021) Recent accomplishments on the synthetic/biological facets of pharmacologically active 1H–1,2,3-triazoles. Eur J Med Chem 212:113069. https://doi.org/10.1016/j.ejmech.2020.113069
24. Shalini K, Sharma PK, Kumar N (2010) Imidazole and its biological activities: a review. Der Chemica Sinica 1(3):36–47
25. Razzaghi-Asl N, Sepehri S, Ebadi A, Karami P, Nejatkhah N, Johari-Ahar M (2020) Insights into the current status of privileged N-heterocycles as antileishmanial agents. Mol Diversity 24(2):525–569. https://doi.org/10.1007/s11030-019-09953-4
26. Deswal L, Verma V, Kumar D, Kaushik Chander P, Kumar A, Deswal Y, Punia S (2020) Synthesis and antidiabetic evaluation of benzimidazole-tethered 1,2,3-triazoles. Arch Pharm 353(9):2000090. https://doi.org/10.1002/ardp.202000090
27. Zawawi NKNA, Taha M, Ahmat N, Ismail NH, Wadood A, Rahim F (2017) Synthesis, molecular docking studies of hybrid benzimidazole as α-glucosidase inhibitor. Bioorg Chem 70:184–191. https://doi.org/10.1016/j.bioorg.2016.12.009
28. Taha M, Rahim F, Zaman K, Selvaraj M, Uddin N, Farooq RK, Nawaz M, Sajid M, Nawaz F, Ibrahim M, Khan KM (2020) Synthesis, α-glycosidase inhibitory potential and molecular docking

study of benzimidazole derivatives. Bioorg Chem 95:103555. https://doi.org/10.1016/j.bioorg.2019.103555
29. Rahim F, Zaman K, Taha M, Ullah H, Ghufran M, Wadood A, Rehman W, Uddin N, Shah SAA, Sajid M, Nawaz F, Khan KM (2020) Synthesis, in vitro alpha-glucosidase inhibitory potential of benzimidazole bearing bis-Schiff bases and their molecular docking study. Bioorg Chem 94:103394. https://doi.org/10.1016/j.bioorg.2019.103394
30. Ye G-J, Lan T, Huang Z-X, Cheng X-N, Cai C-Y, Ding S-M, Xie M-L, Wang B (2019) Design and synthesis of novel xanthone-triazole derivatives as potential antidiabetic agents: α-Glucosidase inhibition and glucose uptake promotion. Eur J Med Chem 177:362–373. https://doi.org/10.1016/j.ejmech.2019.05.045
31. Asemanipoor N, Mohammadi-Khanaposhtani M, Moradi S, Vahidi M, Asadi M, Faramarzi MA, Mahdavi M, Biglar M, Larijani B, Hamedifar H, Hajimiri MH (2020) Synthesis and biological evaluation of new benzimidazole-1,2,3-triazole hybrids as potential α-glucosidase inhibitors. Bioorg Chem 95:103482. https://doi.org/10.1016/j.bioorg.2019.103482
32. Ali M, Khan KM, Salar U, Ashraf M, Taha M, Wadood A, Hamid S, Riaz M, Ali B, Shamim S, Ali F, Perveen S (2018) Synthesis, in vitro $$\alpha $$-glucosidase inhibitory activity, and in silico study of (E)-thiosemicarbazones and (E)-2-(2-(arylmethylene) hydrazinyl)-4-arylthiazole derivatives. Mol Divers 22(4):841–861. https://doi.org/10.1007/s11030-018-9835-2
33. Ali F, Khan KM, Salar U, Taha M, Ismail NH, Wadood A, Riaz M, Perveen S (2017) Hydrazinyl arylthiazole based pyridine scaffolds: synthesis, structural characterization, in vitro α-glucosidase inhibitory activity, and in silico studies. Eur J Med Chem 138:255–272. https://doi.org/10.1016/j.ejmech.2017.06.041
34. Mehrazar M, Hassankalhori M, Toolabi M, Goli F, Moghimi S, Nadri H, Bukhari SNA, Firoozpour L, Foroumadi A (2020) Design and synthesis of benzodiazepine-1, 2, 3-triazole hybrid derivatives as selective butyrylcholinesterase inhibitors. Mol Diversity 24(4):997–1013
35. Turky A, Bayoumi AH, Sherbiny FF, El-Adl K, Abulkhair HS (2021) Unravelling the anticancer potency of 1,2,4-triazole-N-arylamide hybrids through inhibition of STAT3: synthesis and in silico mechanistic studies. Mol Diversity 25(1):403–420. https://doi.org/10.1007/s11030-020-10131-0
36. Yazdani M, Edraki N, Badri R, Khoshneviszadeh M, Iraji A, Firuzi O (2020) 5, 6-Diphenyl triazine-thio methyl triazole hybrid as a new Alzheimer's disease modifying agents. Mol Diversity 24(3):641–654
37. Asgari MS, Mohammadi-Khanaposhtani M, Sharafi Z, Faramarzi MA, Rastegar H, Nasli Esfahani E, Bandarian F, Ranjbar Rashidi P, Rahimi R, Biglar M, Mahdavi M, Larijani B (2021) Design and synthesis of 4,5-diphenyl-imidazol-1,2,3-triazole hybrids as new anti-diabetic agents: in vitro α-glucosidase inhibition, kinetic and docking studies. Mol Divers 25(2):877–888. https://doi.org/10.1007/s11030-020-10072-8
38. Nasli-Esfahani E, Mohammadi-Khanaposhtani M, Rezaei S, Sarrafi Y, Sharafi Z, Samadi N, Faramarzi MA, Bandarian F, Hamedifar H, Larijani B, Hajimiri M, Mahdavi M (2019) A new series of Schiff base derivatives bearing 1,2,3-triazole: design, synthesis, molecular docking, and α-glucosidase inhibition. Arch Pharm 352(8):1900034. https://doi.org/10.1002/ardp.201900034
39. Taslimi P, Turhan K, Türkan F, Karaman HS, Turgut Z, Gulcin I (2020) Cholinesterases, α-glycosidase, and carbonic anhydrase inhibition properties of 1H-pyrazolo [1, 2-b] phthalazine-5, 10-dione derivatives: Synthetic analogues for the treatment of Alzheimer's disease and diabetes mellitus. Bioorgan Chem 97:103647
40. Lolak N, Akocak S, Türkeş C, Taslimi P, Işık M, Beydemir Ş, Gülçin İ, Durgun M (2020) Synthesis, characterization, inhibition effects, and molecular docking studies as acetylcholinesterase, α-glycosidase, and carbonic anhydrase inhibitors of novel benzenesulfonamides incorporating 1, 3, 5-triazine structural motifs. Bioorgan Chem 100:103897
41. Hashmi S, Khan S, Shafiq Z, Taslimi P, Ishaq M, Sadeghian N, Karaman HS, Akhtar N, Islam M, Asari A (2021) Probing 4-(diethylamino)-salicylaldehyde-based thiosemicarbazones as multi-target directed ligands against cholinesterases, carbonic anhydrases and α-glycosidase enzymes. Bioorgan Chem 107:104554
42. Sherafati M, Mohammadi-Khanaposhtani M, Moradi S, Asgari MS, Najafabadipour N, Faramarzi MA, Mahdavi M, Biglar M, Larijani B, Hamedifar H, Hajimiri MH (2020) Design, synthesis and biological evaluation of novel phthalimide-Schiff base-coumarin hybrids as potent α-glucosidase inhibitors. Chem Pap 74(12):4379–4388. https://doi.org/10.1007/s11696-020-01246-7
43. Iftikhar M, Shahnawaz SM, Riaz N, Aziz-ur-Rehman AI, Rahman J, Ashraf M, Sharif MS, Khan SU, Htar TT (2019) A novel five-step synthetic route to 1,3,4-oxadiazole derivatives with potent α-glucosidase inhibitory potential and their in silico studies. Arch Pharm 352(12):1900095. https://doi.org/10.1002/ardp.201900095